ISSN 1726-5749

SENSORS & TRANSDUCERS

vol. 88
2/08

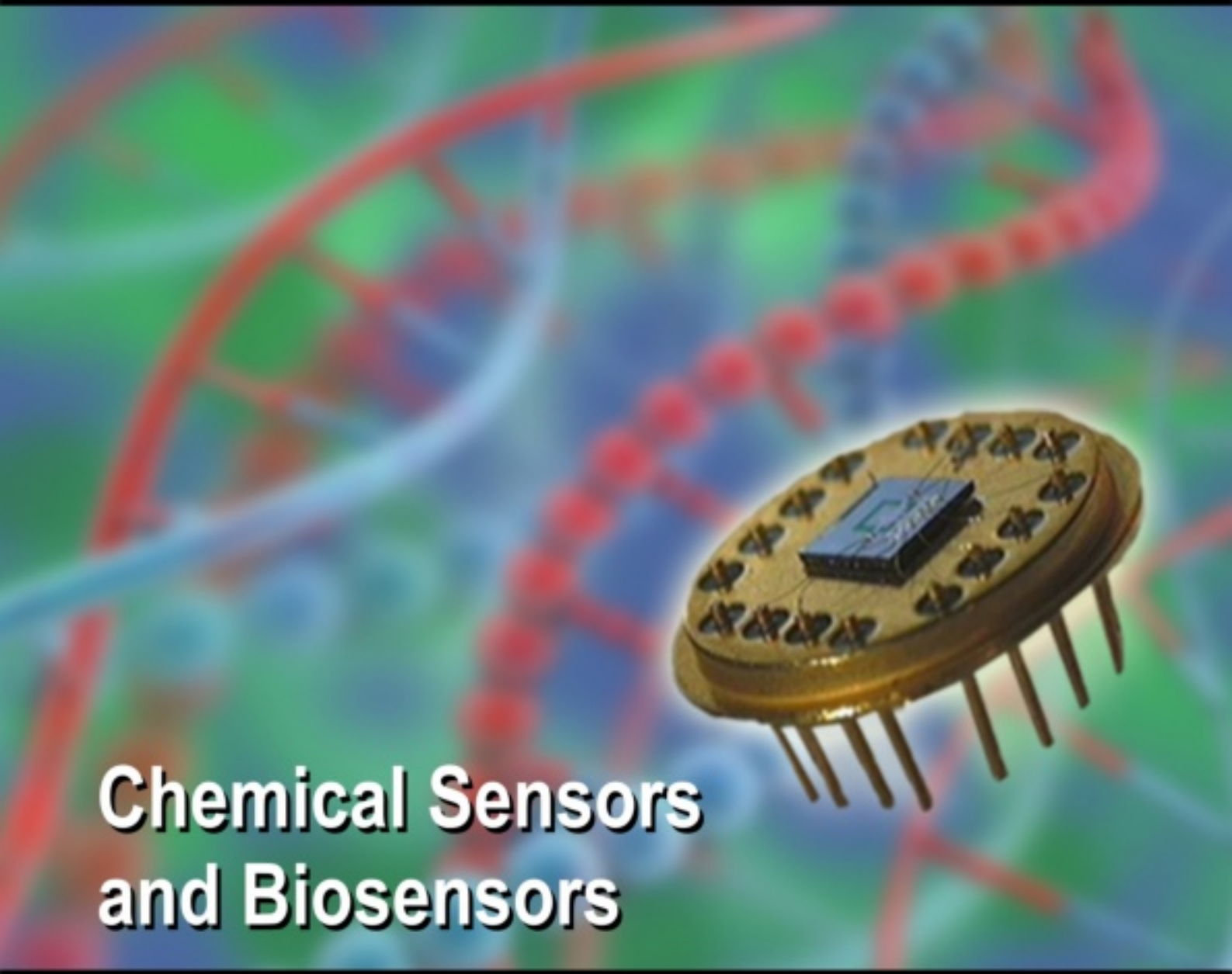

Chemical Sensors and Biosensors

International Frequency Sensor Association Publishing

IFSA

Sensors & Transducers

Volume 88
Issue 2
February 2008

www.sensorsportal.com

ISSN 1726-5479

Sensors & Transducers Journal (ISSN 1726-5479) is a peer review international journal published monthly online by International Frequency Sensor Association (IFSA). Available in electronic and CD-ROM.

Sensors & Transducers Journal

Contents

Volume 88
Issue 2
February 2008

www.sensorsportal.com

ISSN 1726-5479

Research Articles

Confocal Microscopy of Bioconjugated Carbon Nanotubes for Biosensor Applications
Kasif Teker..... 1

A Portable Light-Excitation Equipped Bio-Amperometer for Electrogenic Biomaterials to Support the Technical Development of Most Biosensors
Arianna Tibuzzi, Gianni Pezzotti, Teresa Lavecchia Giuseppina Rea, Maria Teresa Giardi..... 9

Development of a Fiber-Optic Capillary Evanescent Wave Surface Plasmon Resonance Biosensor
Brian K. Keller, Olga Shulga, Christopher P. Palmer, Michael D. Degrandpre..... 21

Improving Probe Immobilization for Label-Free Capacitive Detection of DNA Hybridization on Microfabricated Gold Electrodes
Sandro Carrara, Vijayender Kumar Bhalla, Claudio Stagni, Luca Benini, Bruno Riccò, Bruno Samorì..... 31

Comparative Study of Irradiated And Annealed ZnO Thin Films For Room Temperature Ammonia Gas Sensing
Abhijeet Kshirsagar, Jagdish Deshpande, D. K. Avasthi, T. M. Bhave, S. A. Gangal..... 40

Glutathione Modified Gold Piezoelectric and Voltammetric Sensors for Determination of Mercury in a Wide Concentration Range
Maria Hepel, Julia Dallas and Mark D. Noble..... 47

A Dew Point Meter Comprising a Nanoporous Thin Film Alumina Humidity Sensor with a Linearizing Capacitance Measuring Electronics
Dilip Kumar Ghara, Debdulal Saha and Kamalendu Sengupta..... 59

Solid-State Conductivity of Sucrose and its Applications as Humidity and Temperature Sensors
A. K. Yadav, B. C. Yadav and Kaman Singh..... 66

Sensing Behavior of Sr and Bi Doped LaCoO3 Sensors
G. N. Chaudhary, M. J. Pawar..... 74

Authors are encouraged to submit article in MS Word (doc) and Acrobat (pdf) formats by e-mail: editor@sensorsportal.com
Please visit journal's webpage with preparation instructions: http://www.sensorsportal.com/HTML/DIGEST/Submition.htm

Sensors & Transducers Journal, Vol. 88, Issue 2, February 2008, pp. 21-30

www.sensorsportal.com

Sensors & Transducers

ISSN 1726-5479

http://www.sensorsportal.com

Development of a Fiber-Optic Capillary Evanescent Wave Surface Plasmon Resonance Biosensor

Brian K. KELLER, Olga SHULGA, Christopher P. PALMER, Michael D. DEGRANDPRE

The University of Montana, Department of Chemistry, 32 Campus Drive, Missoula, MT, 59812, USA
E-mail: wavenumber9@hotmail.com, Michael.DeGrandpre@umontana.edu

Received: 31 January 2008 /Accepted: 22 February 2008 /Published: 26 February 2008

Abstract: Development of a surface plasmon resonance (SPR) FOCap (fiber-optic capillary) sensor for bulk and localized refractive index measurements is reported. The FOCap supports multimode light propagation within the capillary wall. An evanescent field, protruding from the capillary wall and into the core, is attenuated by interacting with the surface plasmon oscillations from gold nanoparticles (AuNPs) that are covalently immobilized within the capillary. The FOCap design allows for long pathlength evanescent sensing. The response of the FOCap SPR sensor to bulk refractive index solutions is tested and the optical properties are discussed. The device may also function as a localized refractive index biosensor. Development of a protein-specific biosensor is ongoing but proof-of-concept is confirmed by a non-specific interaction between fibrinogen and a self-assembled monolayer (SAM) covering the AuNP surface. In the future, the FOCap SPR sensor will be tested for sensitivity with biotin-streptavidin affinity and protein specificity will be demonstrated by antibody/antigen affinity interactions. Ultimately this easy-to-assemble SPR biosensor could be utilized in routine protein assays. *Copyright © 2008 IFSA.*

Keywords: Fiber-optic capillary, Capillary waveguide, Surface plasmon resonance, Fiber-optic biosensor

1. Introduction

In recent years there has been much interest in the development and commercialization of SPR-based (surface plasmon resonance) chemical and biochemical sensors [1-5]. Colloidal gold exhibits surface plasmon oscillations when the electric field of excitation light polarizes conduction electrons on the

nanoparticle surface [6-7]. The absorption spectra of gold nanoparticles has bulk absorption and scattering contributions as well as the characteristic visible absorption peak. SPR is very sensitive to changes in refractive index at the metal surface. SPR-based sensors have been developed to detect pesticides [8] and arsenic [9] but biosensing is by far the most common application [10,11]. SPR-based immunosensors utilize anti-body/antigen affinity interactions on nanoparticle surfaces for optical detection. Binding of a large antigen to an anti-body attached to colloidal gold causes a distortion in the TM field at the nanoparticle surface and results in a change in the visible absorption maximum (λ_{max}).

Traditional SPR is measured by ATR (attenuated total reflection) in the Kretschmann configuration using a prism coupler with a metal layer on the reflecting facet. SPR sensing can also be performed on the surface of an optical waveguide. These simple label-free optical biosensors can be easy to fabricate at low costs and with simpler instrumentation compared to prism-based beam-scanning SPR instrumentation. There are several examples of fiber optic-based SPR chemical and biosensors [12-15]. Fiber-optic SPR sensors can be designed to operate in either reflectance or transmittance-based configurations. Typical reflectance configurations have the metal layer placed at the fiber tip, and are often referred to as microprobes. Excitation light travels down the fiber to the tip where reflectance occurs back into the fiber and is directed to a detector through a beamsplitter. Transmittance-based fiber-optic SPR sensors typically utilize evanescent waves to interrogate a metal colloid surface. The colloid is deposited or immobilized onto a clad-removed section of the fiber optic. The guided modes within the fiber are attenuated when the evanescent waves interact with the nanoparticle surface.

A new commercial fiber-optic capillary or FOCap (Polymicro Technologies, LLC) is an ideal waveguide for long-pathlength evanescent sensing. The FOCap construction and its standard method of light propagation are shown in Fig. 1. FOCaps are similar to standard GC capillaries but have an outer clad with refractive index n_3 lower than the wall. Light entering the FOCap wall at ray 1 propagates along trace 1-4 and generates an evanescent wave that penetrates ~ 200 nm deep (with ~500 nm light) into the capillary core at ray 3. Attenuation of the evanescent field occurs when absorbers are present at or near the inner surface. Light entering the core along trace 5-7 quickly exits the waveguide.

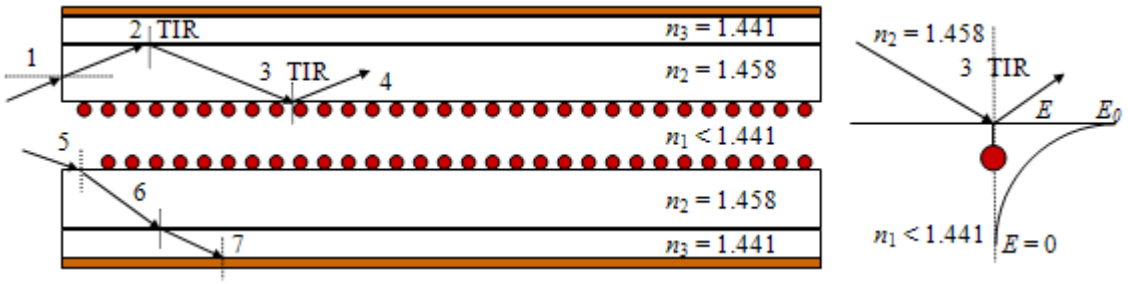

Fig. 1. Cylindrical layers of dielectric media in a FOCap (refractive indicies at right) with immobilized AuNPs attached to the inner wall. When filled with solutions of refractive index $n_1 < 1.441$, light propagates down the FOCap walls and has an evanescent field (at point 3) that penetrates into the capillary core. The evanescent electric field illustrated at the right, decreases exponentially from a maximum E_0 with distance from the capillary wall. Tethered AuNPs within the evanescent field will attenuate the intensity of light propagating down the FOCap wall.

Fiber-optic sensors are limited to a short clad-removed sensing region and also require construction of custom sample cells [16]. The FOCap configuration allows for long-pathlength evanescent sensing. Other FOCap benefits include: a small well-defined sample volume (10-100's of μl), and an inner-protected silica surface that can be easily modified to allow covalent attachment of AuNPs. The

FOCap light-guiding properties have been investigated and some simple sensors have already been developed [17-20]. This report covers some interesting aspects of our recently developed FOCap SPR sensor.

2. Materials and Preparation

Gold nanoparticles (AuNPs) were prepared by citrate reduction of $HAuCl_4$ (hydrogen tetrachloroaurate (III) trihydrate, Sigma-Aldrich, 99.9 %) [21]. A 10 ml aqueous solution of 1 mM $HAuCl_4$ was brought to a boil in a 30 ml beaker with rapid stirring. A 1 ml aqueous solution of 38.8 mM sodium citrate was then added. The solution was boiled for an additional 10 minutes while the color changed from pale yellow to deep ruby red. The AuNP size was estimated by scanning electron microscopy (SEM) as shown in Fig. 2. SEM images were made on porous silica beads (1000 μm diameter) because of difficulties in obtaining images of AuNPs within the FOCap and also on glass slides. The AuNPs were covalently immobilized to the silica beads by first placing them in a 5% solution of 3-mercaptopropyl trimethoxysilane (MPTMS) in water at room temperature for two hours. The silica beads were filtered, washed, and placed in the AuNP colloidal suspension for one hour. The silica beads with AuNPs attached were then rinsed and dried to a glass slide and the SEM analysis was performed. Fig. 2 indicates that the AuNP size varies but the average likely falls somewhere near 20-30 nm in diameter. A statistical analysis of AuNP size by transmission electron microscopy (TEM) is planned [22].

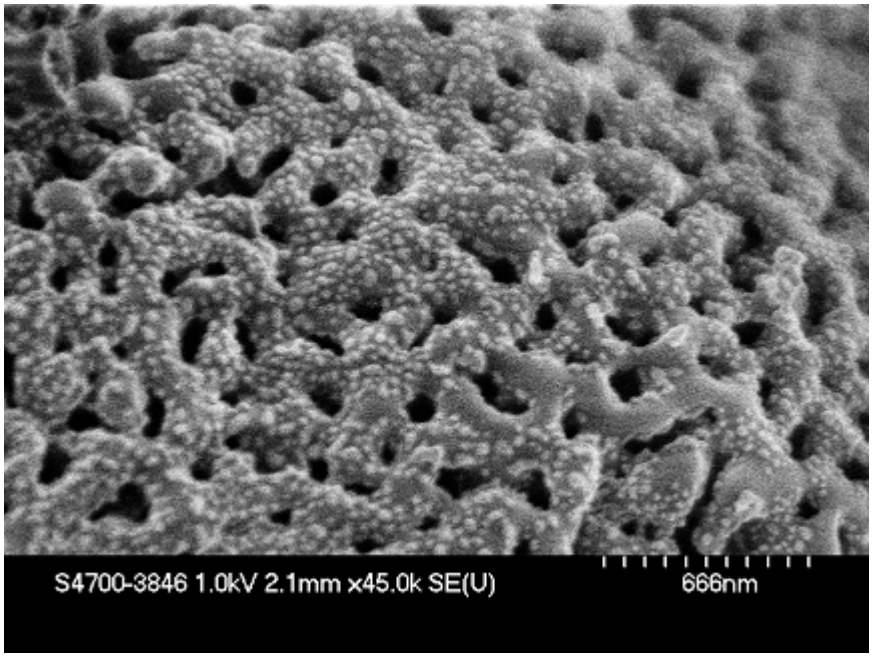

Fig. 2. SEM image of AuNPs on porous fused silica bead indicate ~20-30 nm diameter particle size.

Before AuNP immobilization the FOCap was cleaned with 1 M H_2SO_4, 1 M NaOH, and 10% H_2O_2, in sequence. The capillary was filled with each solution using a syringe and the ends were sealed with a torch. The capillary was then placed in an 80°C water bath for 2 hours. The capillary was flushed with air and filled with the next solution. After cleaning the capillary was rinsed with methanol (HPLC grade) and toluene (HPLC grade) and then filled with a 5% solution of MPTMS in toluene, which was allowed to react for 2 hours at room temperature. The capillary was then rinsed with toluene, methanol, and water, and filled with the AuNP suspension, which was allowed to react with the thiol tether for 12 hours. A self-assembled monolayer of MPA (mercaptopropionic acid) was formed on the

AuNP surface by filling the capillary with a 1 mM solution of MPA in ethanol, which was allowed to react for 10 minutes at room temperature. The capillary with the AuNP-MPA SAM was rinsed with ethanol and was used in the fibrinogen adsorption studies (Fig. 9).

3. Experimental

A schematic of the experimental apparatus used to measure evanescent absorbance from surface plasmons in FOCaps is shown in Fig. 3. This instrument and configuration is explained in more detail elsewhere [18]. A commercial fiber coupler with two light-directing mirrors is installed within the sample area of an Agilent 8453 spectrophotometer. The instrument source light is redirected with a focusing mirror to the endface of an optical fiber mounted in the coupler input barrel. The source light is then directed to the FOCap in a clear polymethacrylate T-union shown in the figure inset. With this instrumental configuration the entire endface of the FOCap is illuminated. However, light guiding only occurs down the capillary walls as shown in Fig. 1. Light passing down the walls of the FOCap is directed to a collecting fiber in a second T-union. The light-collecting barrel is equipped with a lens that directs the throughput light to a flat mirror and then to the spectrophotometer grating and detector. A syringe pump introduces sample solutions into the FOCap through the T-unions and waste is collected after the capillary distill end. Each endface of the FOCap and each fiber end are carefully polished.

Evanescent absorbance spectra of the SPR FOCaps were determined from the ratio of transmitted light intensities of the AuNP-modified FOCap relative to a blank (bare, without AuNPs) FOCap. Blank transmission intensity (I_0) was first measured and recorded in the blank FOCap filled with the solution of interest. Then the AuNP-modified FOCap (same length as blank FOCap) was installed in the T-unions and the transmission intensity (I) was measured in again the same solution. Evanescent absorbance, $-\log(I/I_0)$, was determined manually.

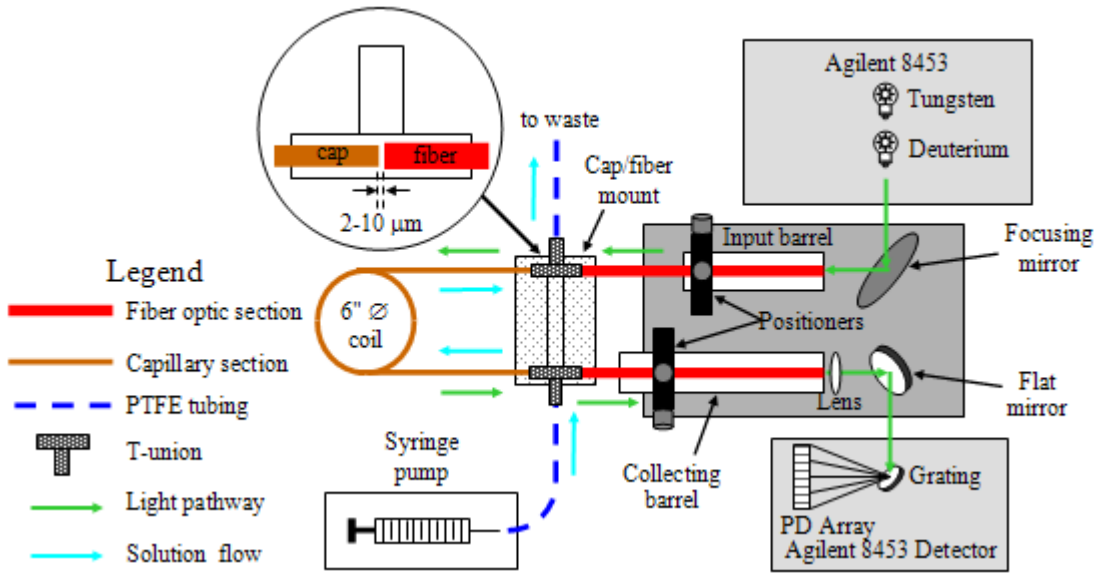

Fig. 3. Diagram of apparatus used to measure evanescent absorbance in FOCaps.

4. Results and Discussion

Fig. 4 shows the UV-Vis absorbance spectra of the AuNP solution in a 1 cm cuvet and the evanescent absorbance spectrum of immobilized AuNPs in a 100 cm long FOCap filled with ethanol. The FOCap spectrum has a larger λ_{max} and is somewhat broader than the cuvet spectrum. The fact that λ_{max} in the FOCap has only slightly increased relative to the suspension suggests that most of the immobilized AuNPs are relatively isolated from one another on the capillary surface. The small change in λ_{max} is likely due to the close proximity of some AuNPs, which results in some plasmon coupling between closely neighboring particles.

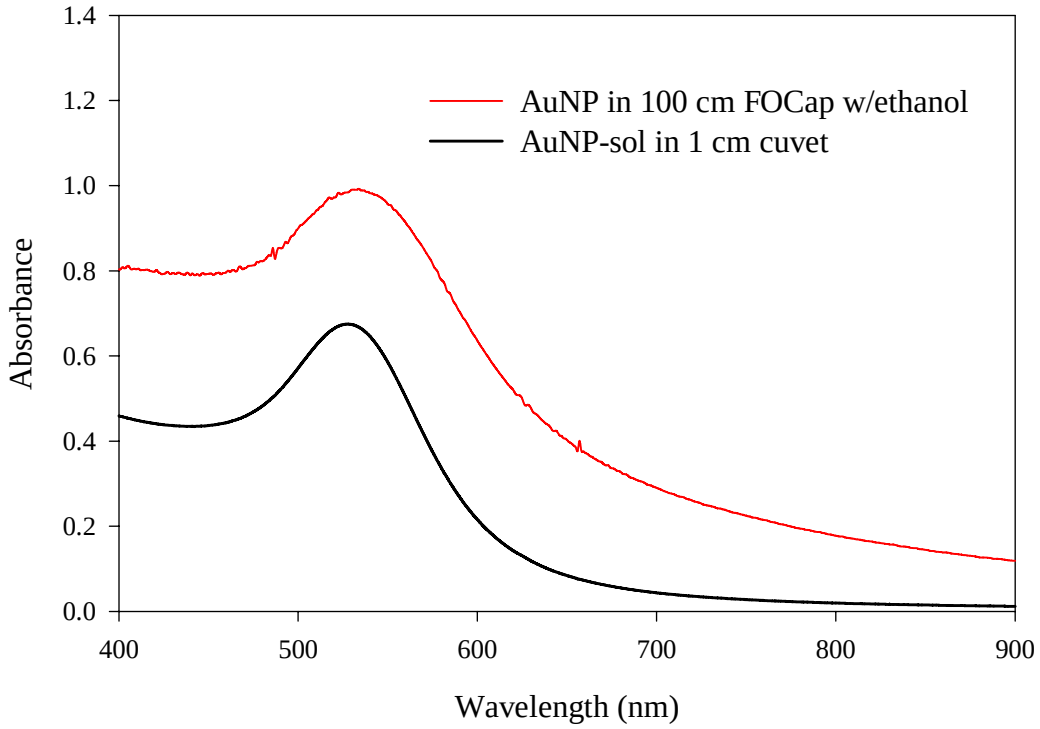

Fig. 4. Absorbance spectrum of AuNP-sol (as prepared in Section 2) in a 1 cm cuvet (black) and the evanescent absorbance spectrum of AuNPs immobilized in a 100 cm long FOCap.

The response of the SPR FOCap to changes in bulk refractive index was first investigated. Fig. 5 shows the results of bulk refractive index testing in a 50 cm long AuNP-modified FOCap. The AuNPs are not covered (no SAM). The bulk refractive index within the FOCap core was varied with solutions of 0-50% sucrose in water. The range of refractive indices of the Brix solutions, from 1.333 to 1.420, was determined with an Abbe refractometer. The evanescent absorbance response to bulk refractive index was determined by first recording blank transmission intensities (I_0) for each Brix solution in a bare FOCap. The AuNP-modified FOCap was then installed into the apparatus and light transmission intensity (I) was measured for each solution. Evanescent absorbance, $-\log(I/I_0)$, was then determined manually. These steps were necessary because the blank transmission intensity in the FOCap increases with bulk refractive index due to refractive index matching that occurs between the input and output optical fibers and each FOCap end in the T-unions (see inset Fig. 3). Evanescent absorbance and λ_{max} from Fig. 5 are plotted in Fig. 6. The dependence of absorbance and λ_{max} are both non-linear. This is due to an increase in the light penetration of lower order modes when the FOCap core bulk refractive index increases. The theoretical curve in Fig. 6 was calculated from the depth of penetration, $d_p = \lambda_{max} / \{2\pi[\sin^2\theta - (n_1/n_2)^2]^{1/2}\}$. The d_p is also wavelength dependant but the changes are very small over the λ_{max} range in Fig. 5.

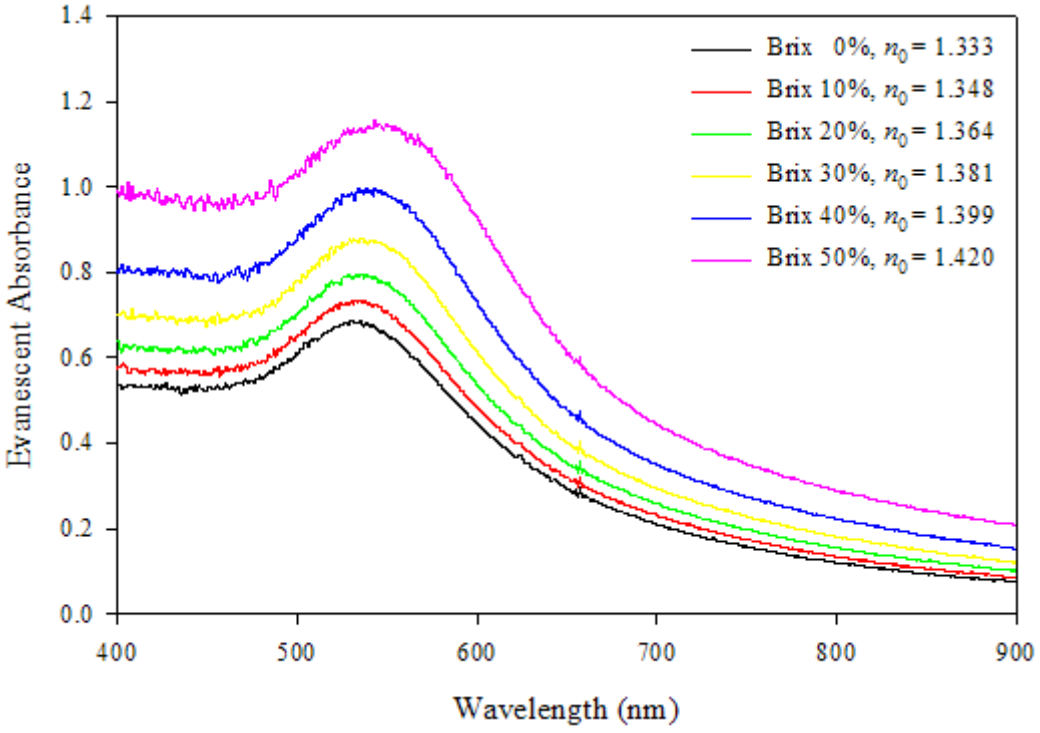

Fig. 5. Evanescent absorbance spectra in a 50 cm long SPR FOCap with increasing bulk refractive index.

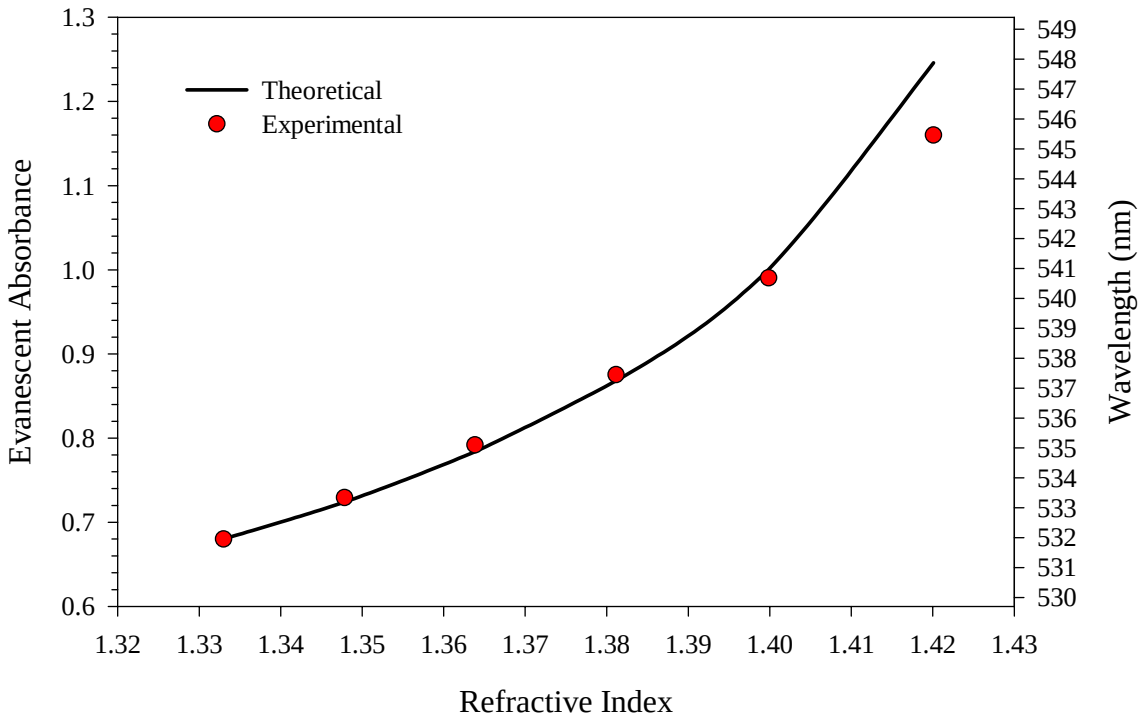

Fig. 6. Evanescent absorbance response of a 50 cm long SPR FOCap with increasing bulk refractive index from n_1 = 1.330 to 1.420.

The dependence of the FOCap SPR sensor was also tested with increasing waveguide physical length and therefore increasing optical pathlength. Nanopure water (n_1 = 1.330) was used to fill each of the FOCaps. Note that λ_{max} does not change in FOCaps up to 100 cm. This confirms that the increase in evanescent absorbance is a pathlength effect and is not due to changes in the bulk refractive index. In FOCaps longer than 100 cm, λ_{max} begins to slightly increase and the absorbance at longer wavelengths increases significantly. The plasmon resonance peak also begins to decrease relative to the bulk absorbance contribution.

Data from Fig. 7 is plotted in Fig. 8. Evanescent absorbance from SPR is linear in FOCaps up to 100 cm in length but begins to curtail in longer FOCaps. There may be two or more contributions to rapid non-linearity in FOCaps over 100 cm. The first is due to the mode distribution of light propagation in the waveguide. It was previously discovered that the mode distribution is heavily weighted in low-order propagating modes [18]. This leads to a pseudo stray light effect because the low order modes have much lower light penetration into the rarer medium than higher order modes. In fact, many of the lowest order modes, which make up a highly significant portion of the mode distribution, may propagate down the FOCap walls with very little penetration power into the capillary core. Non-linear absorbance is likely compounded by the fact that surface plasmon resonance is only excited by TM-polarized light, which makes up only a portion of the source light. This may be partly why the plasmon resonance peak decreases relative to the bulk particle absorbance contribution in FOCaps longer than 100 cm.

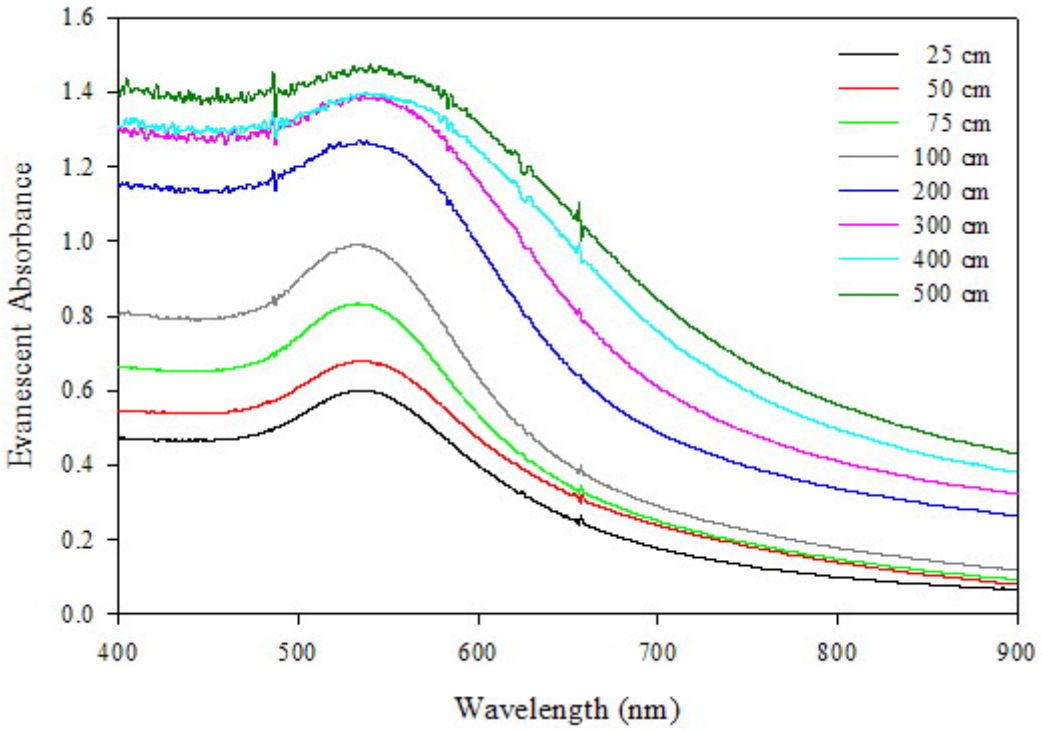

Fig. 7. Evanescent absorbance due to SPR in FOCaps with increasing length to 5 m.

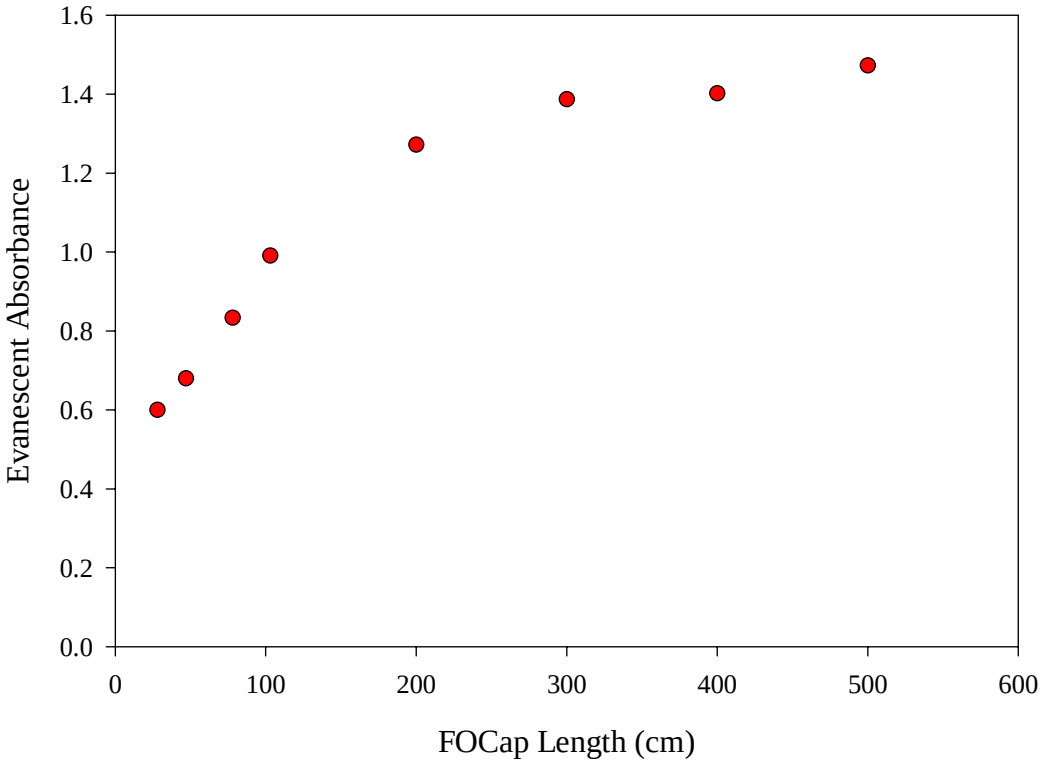

Fig. 8. Evanescent absorbance response in FOCap SPR sensors with increasing length to 5 m.

The basic principles of localized surface plasmon resonance biosensing are illustrated in Fig. 9. We also use this sensing strategy to demonstrate proof-of-concept for the FOCap biosensor in Fig. 10. Colloidal gold was immobilized in the FOCap and the AuNPs are then functionalized with a SAM of MPA as described previously (see Section 2). When a protein, in this case fibrinogen, is injected into the capillary, a biomolecular binding event occurs that results in a change in the localized surface plasmon resonance (LSPR) at the AuNP surface. The change in LSPR increases the absorbance and also λ_{max} of the AuNPs.

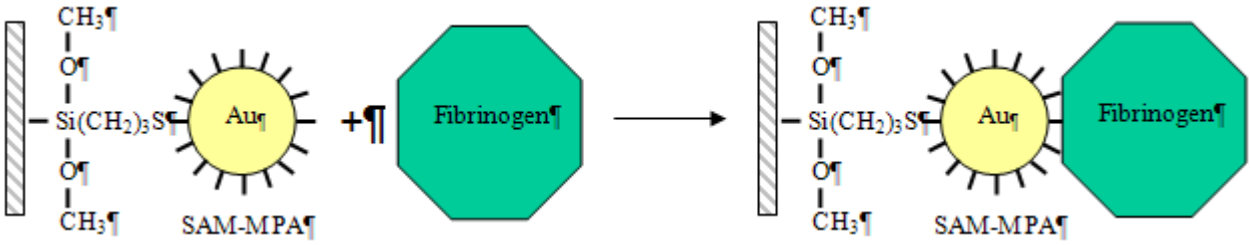

Fig. 9. Binding of a large biomolecule like fibrinogen to a SAM-functionalized AuNP will result in changes in the localized surface plasmon resonance on the AuNP surface.

Proof-of-concept of the FOCap biosensor is demonstrated in Fig. 10. Binding in real time between the SAM carboxylic acid terminal groups and fibrinogen results in a change in the local refractive index and an increase in the evanescent absorbance from AuNP SPR [23]. There are no significant differences in the bulk refractive indices of the three concentrations of fibrinogen (in water) used in Fig. 10.

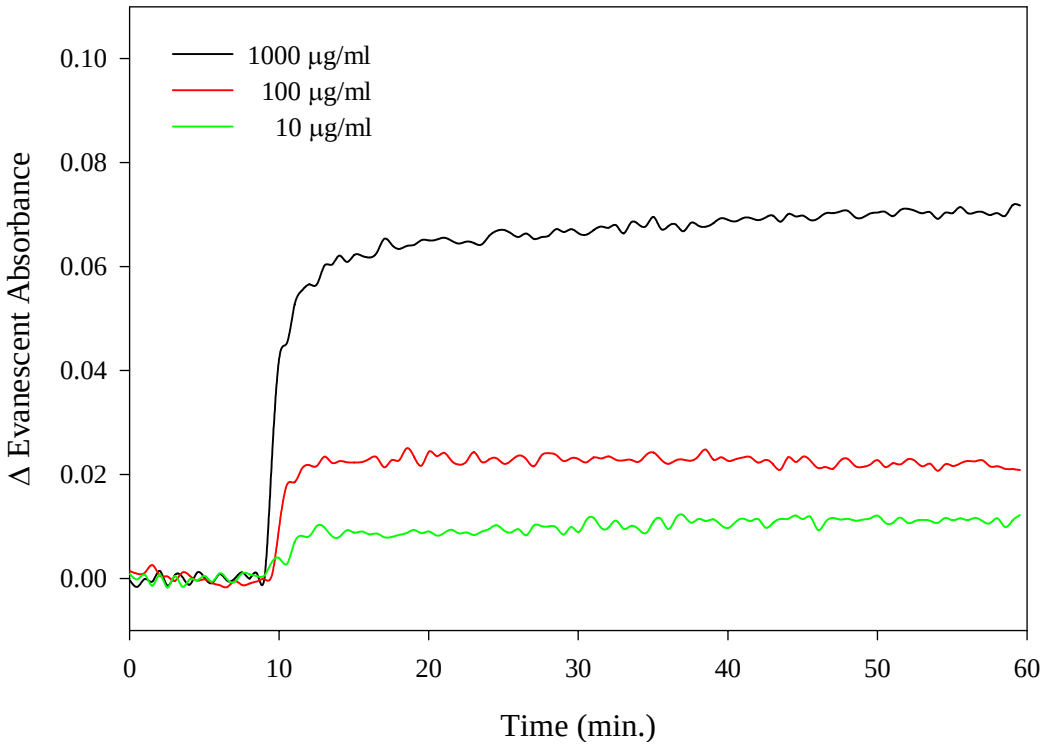

Fig. 10. Evanescent absorbance changes in real time after injection of fibrinogen into a 50 cm FOCap with immobilized AuNPs covered with an MPA-SAM.

5. Conclusions

The optical characteristics of a FOCap utilizing SPR on AuNPs indicate that the waveguide can be developed into a long pathlength evanescent biosensor. The biosensor is easily coupled to a commercial spectrophotometer. Assembly of the FOCap biosensor was relatively simple with low costs. The FOCap construction does not require a custom sample cell like traditional fiber-optic-based SPR sensors. The sensor can detect changes in bulk and localized refractive index. Detection sensitivity will be investigated in the future with biotin-streptavidin affinity.

Acknowledgements

This research was sponsored by the Army Research Laboratory and was accomplished under Cooperative Agreement Number W911NF-04-2-0043. The views and conclusions contained in this document are those of the authors and should not be interpreted as representing the official policies, either expressed or implied, of the Army Research Laboratory or the U.S. Government. The U.S. Government is authorized to reproduce and distribute reprints for Government purposes notwithstanding any copyright notation hereon.

References

[1]. J. Homola, S. S. Yee, G. Gauglitz, Surface plasmon resonance sensors: review, *Sensors and Actuators B: Chemical*, 54, 1999, pp. 3-15.

[2]. M.-C. Daniel, D. Astruc, Gold nanoparticles: Assembly, supramolecular chemistry, quantum-size related properties, and applications toward biology, catalysis, and nanotechnology, *Chemical Reviews*, 104, 2004, pp. 293-346.

[3]. M. Seydack, Nanoparticle labels in immunosensing using optical detection methods, *Biosensors and Bioelectronics*, 20, 2005, pp. 2454-2469.
[4]. D. R. Shankaran, K. V. Gobi, N. Miura, Recent advancements in surface plasmon resonance immunosensors for detection of small molecules of biomedical, food and environmental interest, *Sensors and Actuators B: Chemical*, 121, 2007, pp. 158-177.
[5]. C. R. Yonzon, X. Zhang, J. Zhao, R. P. Van Duyne, Surface-enhanced nanosensors, *Spectroscopy*, 22, 1, 2007, pp. 42-56.
[6]. S. Link, M. A. El-Sayed, Spectral properties and relaxation dynamics of surface plasmon electronic oscillations in gold and silver nanodots and nanorods, *J. Physical Chemistry B*, 103, 1999, pp. 8410-8426.
[7]. S. Link, M. A. El-Sayed, Shape and size dependence of radiative, non-radiative and photothermal properties of gold nanocrystals, *Int. Rev. Phys. Chem*., 19, 2000, pp. 409-453.
[8]. Rajan, S. Chand, B. D. Gupta, Surface plasmon resonance based fiber-optic sensor for the detection of pesticide, *Sensors and Actuators B: Chemical*, 123, 2007, pp. 661-666.
[9]. E. S. Forzani, K. Foley, P. Westerhoff, N. Tao, Detection of arsenic in groundwater using a surface plasmon resonance sensor, *Sensors and Actuators B: Chemical*, 123, 2007, pp. 82-88.
[10]. T. Schalkhammer, Metal nano clusters as transducers for bioaffinity interactions, *Monatshefte für Chemie*, 129, 1998, pp. 1067-1092.
[11]. F. Frederix, J. -M. Friedt, K. -H. Choi, W. Laureyn, A. Campitelli, D. Mondelaers, G. Maes, G. Borghs, Biosensing based on light absorption of nanoscaled gold and silver particles, *Analytical Chemistry*, 75, 2003, pp. 6894-6900.
[12]. R. C. Jorgenson, S. S. Yee, A fiber-optic chemical sensor based on surface plasmon resonance, *Sensors and Actuators B: Chemical*, 12, 1993, pp. 213-220.
[13]. L. D. Maria, M. Martinelli, G. Vegetti, Fiber-optic sensor based on surface plasmon interrogation, *Sensors and Actuators B: Chemical*, 12, 1993, pp. 221-223.
[14]. S.-F. Cheng, L.-K. Chau, Colloidal gold-modified optical fiber for chemical and biochemical sensing, *Analytical Chemistry*, 75, 2003, pp. 16-21.
[15]. L.-K. Chau, Y.-F. Lin, S.-F. Cheng, T.-J. Lin, Fiber-optic chemical and biochemical probes based on localized surface plasmon resonance, *Sensors and Actuators B: Chemical*, 113, 2006, pp. 100-105.
[16]. V. Ruddy, B. D. MacCraith, J. A. Murphy, Evanescent wave absorption spectroscopy using multimode fibers, *J. Applied Physics*, 67, 1990, pp. 6070-6074.
[17]. B. K. Keller, M. D. DeGrandpre, C. P. Palmer, Characterization of long pathlength capillary waveguides for evanescent chemical sensing applications, *Proceedings of SPIE* 5585, 2004, pp. 143-151.
[18]. B. K. Keller, M. D. DeGrandpre, C. P. Palmer, Waveguiding properties of fiber optic capillaries for chemical sensing applications, *Sensors and Actuators B: Chemical*, 125, 2007, pp. 360-371.
[19]. S. Tao, S. Gong, J. C. Fanguy, X. Hu, The application of a light guiding flexible tubular waveguide in evanescent wave absorption optical sensing, *Sensors and Actuators B: Chemical*, 120, 2007, pp. 724-731.
[20]. E. D. Paprocki, B. K. Keller, C. P. Palmer, W. R. Laws, M. D. DeGrandpre, Characterization of long pathlength capillary waveguides for evanescent fluorescence sensing applications, *Sensors and Actuators B: Chemical*, in press.
[21]. K. C. Grabar, R. G. Freeman, M. B. Hommer, M. J. Natan, Preparation and characterization of Au colloid monolayers, *Analytical Chemistry*, 67, 1995, pp. 735-743.
[22]. K. C. Grabar, K. R. Brown, C. D. Keating, S. J. Stranick, S. -L. Tang, M. J. Natan, Nanoscale characterization of gold colloid monolayers: a comparison of four techniques, *Analytical Chemistry*, 69, 1997, pp. 471-477.
[23]. N. Nath, A. Chilkoti, A colorimetric gold nanoparticle sensor to interrogate biomolecular interactions in real time on a surface, *Analytical Chemistry*, 74, 2002, pp. 504-509.
